Volume 1 | Number 1 | Jan 2013 | Pages 1–100

NJC

New Journal of Chemistry
www.rsc.org/njc

A journal for new directions in chemistry

ROYAL SOCIETY OF CHEMISTRY

cnrs

ROYAL SOCIETY OF CHEMISTRY

www.rsc.org/njc

Microwave-assisted synthesis of 6,6′-(aryl(alkyl)methylene)bis(2,4-dialkylphenol) antioxidants catalyzed by multi sulfonated reduced graphene oxide nanosheets in water

Hossein Naeimi,* and Mohsen Golestanzadeh

Department of Organic Chemistry, Faculty of Chemistry, University of Kashan, Kashan, 87317, I. R. Iran

Email: naeimi@kashanu.ac.ir Tel: +98(31)55912388 Fax: +98(31)55912397

Abstract

Sulfonated reduced graphene oxide nanosheets (RGO-SO₃H) were characterized by field emission scanning electron microscopy (FESEM), transmission electron microscopy (TEM), atomic force microscopy (AFM), Fourier transform infrared spectroscopy (FT-IR), Raman spectroscopy, X-ray diffraction (XRD), thermogravimetric analysis (TGA), and acid-base titration. Multi SO_3H supported on reduced graphene oxide nanosheets was found to be an efficient catalyst for green synthesis of 6,6′-(aryl(alkyl)methylene)bis(2,4-dialkylphenol) Derivatives from 2,4-dialkylphenols and aromatic and aliphatic aldehydes in aqueous media under microwave irradiation. The synthesis of 6,6′-(aryl(alkyl)methylene)bis(2,4-dialkylphenol) Derivatives were carried out in the presence of catalytic amount of the RGO-SO₃H, under thermal and microwave conditions to afford the desired products in high and excellent yields respectively. In addition, the catalyst could be recovered easily and reused several times without any considerable loss of its catalytic activity.

Keywords: Graphene; antioxidants; green Synthesis; microwave; heterogeneous catalyst

Introduction

The phenolic compounds, especially polyphenols have become an intense focus of research interest because of their perceived health-beneficial effects, such as anti-carcinogenic, anti-atherogenic, anti-inflammatory, and anti-microbial activities.[1-3] The phenol structural unit is an important component in many natural products, pharmaceuticals, catalysts and advanced materials.[4, 5] The hydroxyl groups in these materials are responsible for their specific activity.[6-8] Some important and biologically active phenol-based compounds (Figure 1) [9, 10] act as efficient free radicals scavengers by donating their alcoholic hydrogen or one of their delocalized electrons. These compounds are employed in the food industry, in propellant and explosive materials and in other areas as effective antioxidants.
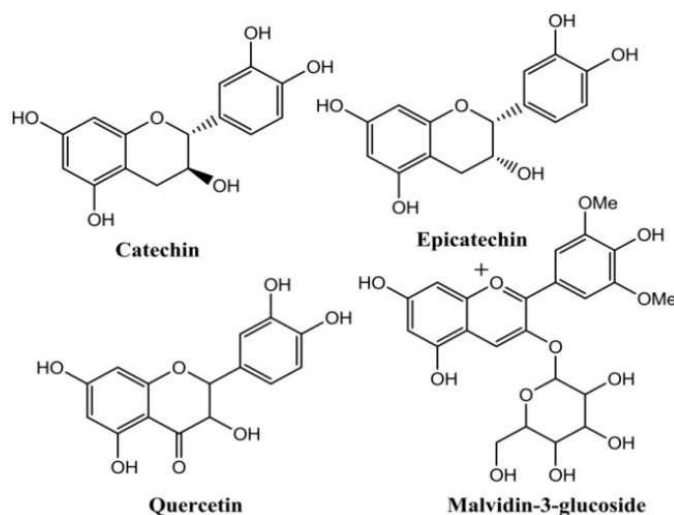
Figure 1. Examples of biologically, and antioxidantly active compounds based phenol.

Owing to the wide application and significance of bisphenolic antioxidants, there is considerable interest in the synthesis of these compounds catalyzed by different homogeneous and heterogeneous catalysts.[11-24] Although each of these protocols has its advantages some of them often suffer from one or more disadvantages. Low yields, long reaction times, tedious work-up

processes, use of hazardous organic solvent, and non-reusable catalytic system are most important deficiencies associated with these methods.

Acid catalyzed chemical processes are widely employed in the organic synthesis to produce different chemicals.[25] In terms of green chemistry, it is very important to replace liquid acid catalysts such as HF, HCl, and H_2SO_4 with solid acid catalysts in organic synthesis.[26-28] Graphene is one of typical support for preparation of heterogeneous catalysts. Graphene possesses a large specific surface area, open porous structure, flexibility, chemical and thermal stability, non-toxicity, wet ability, and very high electrical conductivity, which warrant it as a good candidate support for preparation of heterogeneous catalysts.[29-34] Also, graphene oxide and reduced graphene oxide were employed in the area of scientific works such as sensors,[35, 36] supercapacitors,[37] and photocatalyst.[38, 39]

In last two decades, several reactions have been occurred in the presence of solid catalysts for potential application of microwave irradiation in organic synthesis.[40, 41] In contrast microwave irradiation when a conventional thermal method was employed, catalytic activity of solid heterogeneous catalyst is low.[40] Since the materials and catalyst are directly heated under microwave irradiation without the need for heat transfer, the reaction time is remarkably shortened. Consequently, alternative heating and strict temperature control of a catalyst are some of the features of the reaction catalyzed by a solid catalyst when exposed to microwave irradiation.

Due to the importance of the described compounds, and in continuation of our previous study on preparation of heterogeneous catalytic systems and microwave irradiation,[42-50] herein, we hope

to present the RGO-SO$_3$H as a heterogeneous catalyst for the preparation of 6,6′-(aryl(alkyl)methylene)bis(2,4-dialkylphenol) antioxidants in water under microwave irradiation.

Experimental Section

Materials and apparatus

The chemical and materials used in this research were purchased from Merck chemical company and used without purification. The IR spectra were obtained as KBr pellets in the range of 400-4000 cm^{-1} on a Perkin-Elmer 781 spectrophotometer. The ^{1}H NMR and ^{13}C NMR spectra were recorded in dimethyl sulfoxide (DMSO)-(d$_6$) solvent on a Brucker DRX-400 MHz spectrometer using tetramethylsilane (TMS) as an internal standard. The crystallographic structure of prepared catalyst was investigated on a Philips instrument with 1.54 Å wavelengths of X-ray beam and Cu anode material, at a scanning speed of 2° min^{-1} from 10° to 80° (2θ). The elemental analyses (C, H, N) were obtained from a Carlo ERBA Model EA 1108 analyzer. The Microwave conditions were carried out in microwave oven specially designed for organic synthesis (Milestone LAVIS Basic Microwave). Thermogravimetric analysis (TGA) was performed on a mettler TA4000 system TG-50 at a heating rate of 10 K min^{-1} under N$_2$ atmosphere. The Raman spectra were recorded with an Almega Thermo Nicolet Dispersive Raman spectrometer excited at 532 nm. The morphology of the catalyst was characterized by FESEM Hitachi S4160 instrument. The TEM images were recorded by a Zeiss-EM10C with an acceleration voltage of 80 kV. The AFM image of GO nanosheets and RGO-SO$_3$H were measured using a scanning probe microscope (SPM-9600, Shimadzu). Melting points was obtained with a Yanagimoto micro melting point apparatus and are uncorrected. The purity determination of the substrates and reaction monitoring were accomplished by TLC on silica-gel polygram SILG/UV 254 plates (from Merck Company).

4

Preparation of graphene oxide nanosheets

The GO nanosheets were prepared from natural graphite by the modified Hummer's method.[51] Typically, 5.0 g of natural graphite powder and 2.5 g of sodium nitrate were mixed with 115 mL of sulfuric acid (98%) in a 1000 mL round-bottom flask equipped with a magnetic stirrer and condenser place in an ice bath. The obtained solution was stirred and slowly added 15.0 g of potassium permangenate, and the stirring was continued for 2 h. The mixture solution was transferred to a water bath (35 ^{o}C) and stirred for 30 min. After this step, 230 mL of deionized water was slowly added into the solution and the solution temperature monitored was about 98 °C and stirred for 15 min. Then, 700 mL of deionized water and 50 mL of H_2O_2 (30%) were sequentially added to the mixture solution to terminate the reaction. The resulting materials was filtered and washed with 5% HCl solution followed by distilled water for several times. The solution was filtered under reduced pressure by vacuum pump over sinter-glass (G4). After drying in vacuum at 60 °C for 12 h, the graphite oxide powder was obtained. The graphite oxide was dispersed in distilled water to make concentration of 0.5 mg mL^{-1}, and exfoliated by ultrasound (45 w) for 30 min to generate GO nanosheets, followed by centrifugation at 3500 rpm for 30 min to remove un-exfoliated graphite oxide.

Preparation of reduced graphene oxide nanosheets

First, reduced graphene oxide (RGO) was synthesized by the chemical reduction of GO using $NaBH_4$ as a reducing agent. In a 1000 mL round-bottom flask, 1.0 g of the GO dispersion was added into deionized water (700 mL), followed by sonication (40 w) for 15 min. Then, 2.4 g of $NaBH_4$ was added into the round-bottom flask, heating at 100 °C for 24 h. After this step, the resulted product was washed with water several times and filtered under reduced pressure by

5

vacuum pump over sinter glass (G4) and centrifugation at 3500 rpm for 15 min to obtain RGO

nanosheets.

Preparation of sulfonated reduced graphene oxide nanosheets

The RGO-SO$_3$H was prepared from the hydrothermal sulfonation of RGO using H$_2$SO$_4$ (100 %)

at 180 °C. 1.0 g of RGO was added into 50 mL of H$_2$SO$_4$. After sonication (40 w) for 15 min, the

mixture was transferred into a round-bottom flask under nitrogen atmosphere and stirring to heat

at 180 °C for 24 h. Then, the prepared catalyst was washed with a large amount of deionized

water and drying at 80 °C for 12 h. Finally RGO-SO$_3$H was obtained and employed in the

synthesis of bisphenolic antioxidants.

Procedure for pH analysis of prepared catalyst

The density of sulfonated group on RGO, and GO was calculated by back acid-base titration and

aqueous solution of NaCl. First, 100 mg of RGO-SO$_3$H was sonicated in a water bath for 10 min

under nitrogen atmosphere to degas CO$_2$. Next 10 mL of NaOH 0.098 N was added and the

mixture stirred for 2 h at room temperature. Subsequently, the mixture was filtered through

sintered glass (G-4) and washed several times with deionized water. The filtrate was then titrated

with HCl 0.1 N until reaching the neutral point as monitored by phenolphthalein as indicator.

The volume required to reach the neutral point was substracted from the initial volume of NaOH

used to obtain the volume of NaOH which has reacted with sulfonated group on RGO. In

addition, by the solution of NaCl, the total density of sulfonated groups was measured. To an

aqueous solution of NaCl (1 M, 25 mL) with the primary pH 6.11, the catalyst (100 mg) was

added, and the resulting mixture was stirred for 4 h. Then, pH of the solution was measured.

General procedure for the preparation of bisphenolic antioxidants catalyzed by RGO-SO₃H under thermal conditions

In a 25 mL round-bottom flask equipped with a magnetic bar and condenser, a mixture of 2,4-dialkylphenol (6 mmol), aromatic and aliphatic aldehyde (2 mmol) and RGO-SO₃H (40 mg) was heated at 100 °C under solvent free conditions for appropriate time according to Table 2. The progress of the reaction was monitored by thin layer chromatography (TLC) (*n*-hexane: ethyl acetate 10:4). At the end of the reaction, the mixture was cooled to the room temperature and 15 mL of acetone (3×5 mL) was added. The RGO-SO₃H was filtered under reduced pressure using vacuum pump over sinter glass (G4). The solution was recovered by evaporation on a rotary evaporator. After that, the solid materials were washed with *n*-hexane (5 mL) and deionized water, successively, to afford the pure products. The desired products were kept in an oven at 80 °C for 12 h.

General procedure for the preparation of bisphenolic antioxidants catalyzed by RGO-SO₃H under microwave irradiation

A mixture of 2,4-dialkylphenol (6 mmol), aromatic and aliphatic aldehyde (2 mmol), RGO-SO₃H (30 mg), and water (5 mL) as a green solvent in an open tall beaker was irradiated inside microwave oven at 300 W for the appropriate time. The progress of the reaction was monitored by TLC (*n*-hexane: ethyl acetate 10:4). After completion of the reaction, the mixture was cooled to room temperature and 20 mL of acetone (4×5 mL) was added. The RGO-SO₃H was filtered under reduced pressure using vacuum pump over sinter glass (G4). The solution was recovered by evaporation on a rotary evaporator. After that, the solid materials were washed with *n*-hexane

(5 mL) and deionized water, successively, to afford the pure products. The desired products were kept in an oven at 80 $^{\circ}$C for 12 h.

Procedure for recovery and reusability of the catalyst

Reusability of the RGO-SO$_3$H was studied in the reaction of 2,4-dimethylphenol and 4-bromobenzaldehyde. At the end of each cycle, the catalyst was separated by filtration, washed exhaustively with deionized water, *n*-hexane, and ethanol, then dried at 100 $^{\circ}$C for 12 h before being used with fresh 2,4-dimethylphenol and 4-bromobenzaldehyde. The catalyst can be reused seven cycles under microwave irradiation without any reduction in its catalytic activity.

Spectroscopic and physical data

6,6′-((4-nitrophenyl)methylene)bis(2,4-dimethylphenol) (Table 2, Compound **3a**): mp: 136-138 °C; IR (KBr): ν (cm^{-1}) 3482, 3249, 2958, 1599, 1522, 1475, 1349, 1292, 1113, 879. ^{1}H NMR (400 MHz, DMSO-d$_6$/TMS) δ(ppm): 1.95 (6H, s, Me), 2.47 (6H, s, Me), 6.22 (1H, s, Ar$_3$CH), 6.26 (2H, s, OH), 6.75 (2H, s, 3-H DMP), 7.21 (2H, d, *J=8 Hz*, 2,6-H aldehyde), 8.09 (2H, s, 5-H DMP), 8.11 (2H, d, *J=8 Hz*, 3,5-H aldehyde). Anal. Calcd for C$_{23}$H$_{23}$NO$_4$: C, 73.19; H, 6.14; N, 3.71%. Found: C, 73.06; H, 6.12; N, 3.70%.

6,6′-((3-nitrophenyl)methylene)bis(2,4-dimethylphenol) (Table 2, Compound **3b**): mp: 141-143 °C; IR (KBr): ν (cm^{-1}) 3433, 3082, 2916, 1606, 1525, 1481, 1347, 1217, 1096, 861. ^{1}H NMR (400 MHz, DMSO-d$_6$/TMS) δ(ppm): 1.91 (6H, s,Me), 2.46 (6H, s, Me), 6.24 (1H, s, Ar$_3$CH), 6.28 (2H, s, OH), 6.57 (2H, s, 3-H DMP), 6.75 (1H, d, *J=7.8 Hz*, 5-H aldehyde), 7.43 (1H, d, 6-H aldehyde), 7.53 (2H, d, *J=7.8 Hz*, 2,4-H aldehyde), 7.73 (2H, s, 5-H DMP). Anal. Calcd for C$_{23}$H$_{23}$NO$_4$: C, 73.19; H, 6.14; N, 3.71%. Found: C, 73.21; H, 7.05; N, 3.67%.

6,6′-((4-chlorophenyl)methylene)bis(2,4-dimethylphenol) (Table 2, Compound **3c**): mp: 158-160 °C; IR (KBr): ν (cm^{-1}) 3498, 3467, 3018, 2918, 1587, 1472, 1381, 1254, 1183, 1048, 862. ^{1}H NMR (400 MHz, DMSO-d$_6$/TMS) δ(ppm): 2.03 (6H, s, Me), 2.08 (6H, s, Me), 6.10 (1H, s, Ar$_3$CH), 6.26 (2H, s, OH), 6.71 (2H, s, 3-H DMP), 6.96 (2H, d, *J=7.9 Hz*, 2,6-H aldehyde), 7.28 (2H, s, 5-H DMP), 7.97 (2H, d, *J=7.9 Hz*, 3,5-H aldehyde). Anal. Calcd for C$_{23}$H$_{23}$ClO$_2$: C, 75.30; H, 6.32%. Found: C, 75.19; H, 6.29%.

6,6′-((2-chlorophenyl)methylene)bis(2,4-dimethylphenol) (Table 2, Compound **3d**): mp: 191-193 °C; IR (KBr): ν (cm^{-1}) 3482, 2918, 1600, 1598, 1474, 1331, 1291, 1190, 1037, 866. ^{1}H NMR (400 MHz, DMSO-d$_6$/TMS) δ(ppm): 1.93 (6H, s, Me), 2.08 (6H, s, Me), 6.19 (2H, s, OH), 6.40 (1H, s, Ar$_3$CH), 6.71 (2H, s, 3-H DMP), 6.83 (1H, t, *J=8 Hz*, 4-H aldehyde), 7.18 (2H, s, 5-H DMP), 7.35 (1H, d, *J=7.7 Hz*, 6-H aldehyde), 7.96 (2H, d, 3,5-H aldehyde). Anal. Calcd for C$_{23}$H$_{23}$ClO$_2$: C, 75.30; H, 6.32%. Found: C, 75.29; H, 6.34%.

6,6′-((2,4-dichlorophenyl)methylene)bis(2,4-dimethylphenol) (Table 2, Compound **3e**): mp: 183-185 °C; IR (KBr): ν (cm^{-1}) 3500, 3466, 3022, 2917, 1602, 1481, 1405, 1252, 1184, 1138, 847. ^{1}H NMR (400 MHz, DMSO-d$_6$/TMS) δ(ppm): 1.92 (6H, s, Me), 2.08 (6H, s, Me), 6.17 (2H, s, OH), 6.33 (1H, s, Ar$_3$CH), 6.73 (2H, s, 3-H DMP), 7.80 (2H, s, 5-H DMP), 7.29 (1H, d, *J=8 Hz*, 6-H aldehyde), 7.50 (1H, d, *J=8 Hz*, 5-H aldehyde), 8.01 (1H, s, 2H aldehyde). Anal. Calcd for C$_{23}$H$_{22}$Cl$_2$O$_2$: C, 68.83; H, 5.53%. Found: C, 68.64; H, 5.49%.

6,6′-((2-fluorophenyl)methylene)bis(2,4-dimethylphenol) (Table 2, Compound **3f**): mp: 146-148 °C; IR (KBr): ν (cm^{-1}) 3484, 3920, 1584, 1482, 1333, 1290, 1223, 1193, 1140, 866. ^{1}H NMR (400 MHz, DMSO-d$_6$/TMS) δ(ppm): 1.95 (6H, s, Me), 2.09 (6H, s, Me), 6.26 (2H, s, OH), 6.35 (1H, s, Ar$_3$CH), 6.72 (2H, s, 3-H DMP), 6.72 (1H, t, *J=7.8 Hz*, 4-H aldehyde), 7.06 (2H, s,

5-H DMP), 7.20 (1H, d, *J=8 Hz*, 6-H aldehyde), 7.98 (2H, d, t, 3,5-H aldehyde). ^{13}C NMR (100 MHz, DMSO-d$_6$/TMS) δ(ppm): 17.18, 20.95, 36.84, 115.28, 115.50, 124.44, 127.42, 128.15, 129.80, 130.88, 131.98, 132.13, 150.64, 159.51, and 161.94. Anal. Calcd for C$_{23}$H$_{23}$FO$_2$: C, 78.83; H, 6.62%. Found: C, 78.72; H, 6.61%.

6,6′-((3-fluorophenyl)methylene)bis(2,4-dimethylphenol) (Table 2, Compound **3g**): mp: 94-96 °C; IR (KBr): ν (cm^{-1}) 3335, 3923, 1611, 1586, 1482, 1442, 1385, 1292, 1189, 1142, 783. ^{1}H NMR (400 MHz, DMSO-d$_6$/TMS) δ(ppm): 1.95 (6H, s, Me), 2.09 (6H, s, Me), 6.14 (1H, s, Ar$_3$CH), 6.28 (2H, s, OH), 6.66 (2H, s, 3-H DMP), 6.72 (2H, d, *J=7.9 Hz*, 5,6-H aldehyde), 6.96 (1H, d, *J=7.9 Hz*, 2-H aldehyde), 7.25 (1H, d, *J=7.9 Hz*, 4-H aldehyde), 8.00 (2H, s, 5-H DMP). Anal. Calcd for C$_{23}$H$_{23}$FO$_2$: C, 78.83; H, 6.62%. Found: C, 78.79; H, 6.54%.

6,6′-((4-bromophenyl)methylene)bis(2,4-dimethylphenol) (Table 2, Compound **3h**): mp: >240 °C; IR (KBr): ν (cm^{-1}) 3468, 2917, 1601, 1480, 1401, 1251, 1184, 1138, 1072, 860. ^{1}H NMR (400 MHz, DMSO-d$_6$/TMS) δ(ppm): 2.06 (6H, s, Me), 2.08 (6H, s, Me), 6.07 (1H, s, Ar$_3$CH), 6.25 (2H, s, OH), 6.70 (2H, s, 3-H DMP), 6.88 (2H, d, *J=7.9 Hz*, 2,6-H aldehyde), 7.38 (2H, s, 5-H DMP), 7.96 (2H, d, *J=7.9 Hz*, 3,5-H aldehyde). Anal. Calcd for C$_{23}$H$_{23}$BrO$_2$: C, 67.16; H, 5.64%. Found: C, 67.18; H, 5.61%.

6,6′-((3-bromophenyl)methylene)bis(2,4-dimethylphenol) (Table 2, Compound **3i**): mp: 124-126 °C; IR (KBr): ν (cm^{-1}) 3345, 2922, 1591, 1478, 1383, 1325, 1293, 1188, 1143, 1075, 863. ^{1}H NMR (400 MHz, DMSO-d$_6$/TMS) δ(ppm): 2.03 (6H, s, Me), 2.08 (6H, s, Me), 6.10 (1H, s, Ar$_3$CH), 6.26 (2H, s, OH), 6.72 (2H, s, 3-H DMP), 6.96 (1H, d, *J=8 Hz*, 6-H aldehyde), 7.19 (1H, d, *J=8 Hz*, 5-H aldehyde), 7.21 (1H, *J=7.8 Hz,* 4-H aldehyde), 7.33 (1H, *J=7.8 Hz,* 2-H aldehyde), 8.01 (2H, s, 5-H DMP). ^{13}C NMR (100 MHz, DMSO-d$_6$/TMS) δ(ppm): 17.19, 20.94,

43.50, 121.84, 124.65, 127.57, 128.07, 128.73, 128.98, 129.86, 130.57, 130.94, 131.98, 148.06, and 150.68. Anal. Calcd for $C_{23}H_{23}BrO_2$: C, 67.16; H, 5.64%. Found: C, 67.08; H, 5.51%.

6,6′-((2-bromophenyl)methylene)bis(2,4-dimethylphenol) (Table 2, Compound **3j**): mp: 188-190 °C; IR (KBr): ν (cm^{-1}) 3484, 2917, 1597, 1566, 1474, 1330, 1189, 1140, 1023, 866, 750. ^{1}H NMR (400 MHz, DMSO-d$_6$/TMS) δ(ppm): 1.94 (6H, s, Me), 2.09 (6H, s, Me), 6.18 (2H, s, OH), 6.35 (1H, s, Ar$_3$CH), 6.72 (2H, s, 3-H DMP), 6.83 (1H, d, *J=8 Hz*, 6-H aldehyde), 7.08 (1H, d, *J=8 Hz*, 4-H aldehyde), 7.21 (1H, d, *J=7.7Hz*, 3-H aldehyde), 7.53 (1H, t, *J=7.7Hz*, 5-H aldehyde), 7.97 (2H, s, 5-H DMP). Anal. Calcd for $C_{23}H_{23}BrO_2$: C, 67.16; H, 5.64%. Found: C, 67.20; H, 5.59%.

6,6′-((phenyl)methylene)bis(2,4-dimethylphenol) (Table 2, Compound **3k**): mp: 113-115 °C; IR (KBr): ν (cm^{-1}) 3339, 3021, 2920, 1600, 1481, 1447, 1384, 1292, 1186, 1142, 864, 702. ^{1}H NMR (400 MHz, DMSO-d$_6$/TMS) δ(ppm): 2.06 (6H, s, Me), 2.08 (6H, s, Me), 6.13 (1H, s, Ar$_3$CH), 6.29 (2H, s, OH), 6.70 (2H, s, 3-H DMP), 6.97 (2H, t, *J=8 Hz*, 3,5-H aldehyde), 7.11 (1H, t, *J=8 Hz*, 4-H aldehyde), 7.23 (2H, d, *J=8 Hz*, 2,6-H aldehyde), 7.93 (2H, s, 5-H DMP). Anal. Calcd for $C_{23}H_{24}O_2$: C, 83.10; H, 7.28%. Found: C, 83.14; H, 7.24%.

6,6′-((4-methylphenyl)methylene)bis(2,4-dimethylphenol) (Table 2, Compound **3l**): mp: 168-170 °C; IR (KBr): ν (cm^{-1}) 3501, 2917, 1604, 1476, 1330, 1188, 1139, 1031, 866. ^{1}H NMR (400 MHz, DMSO-d$_6$/TMS) δ(ppm): 2.01 (6H, s, Me), 2.07 (6H, s, Me), 2.21 (3H, s, CH$_3$-aldehyde), 6.06 (1H, s, Ar$_3$CH), 6.28 (2H, s, OH), 6.68 (2H, s, 3-H DMP), 6.84 (2H, d, *J=8.1 Hz*, 3,5-H aldehyde), 7.01 (2H, s, 5-H DMP), 7.88 (2H, d, *J=8.1 Hz*, 2,6-H aldehyde). ^{13}C NMR (100 MHz, DMSO-d$_6$/TMS) δ(ppm): 17.21, 20.97, 43.26, 124.38, 127.30, 128.18, 128.94, 129.45, 129.58,

131.95, 134.81, 141.78, and 150.69. Anal. Calcd for $C_{24}H_{26}O_2$: C, 83.20; H, 7.56%. Found: C, 83.14; H, 7.49%.

6,6′-((3-methoxyphenyl)methylene)bis(2,4-dimethylphenol) (Table 2, Compound **3m**): mp: >270 °C; IR (KBr): ν (cm^{-1}) 3453, 2975, 1622, 1505, 1402, 1347, 1230, 1088, 790. ^{1}H NMR (400 MHz, DMSO-d$_6$/TMS) δ(ppm): 1.94 (6H, s, Me), 2.08 (6H, s, Me), 3.80 (3H, s, OCH$_3$), 6.14 (1H, s, Ar$_3$CH), 6.28 (2H, s, OH), 6.68 (2H, s, 3-H DMP), 6.84 (1H, s, 2-H aldehyde), 6.94 (1H, d, *J=7.9 Hz*, 4-H aldehyde), 7.64 (2H, s, 5-H DMP), 8.12 (2H, m, 5,6-H aldehyde). Anal. Calcd for $C_{24}H_{26}O_3$: C, 79.53; H, 7.23%. Found: C, 79.58; H, 7.20%.

6,6′,6″,6‴-(1,4-phenylenebis(methanetriyl))tetrakis(2,4-dimethylphenol) (Table 2, Compound **3n**): mp: 65-67 °C; IR (KBr): ν (cm^{-1}) 3429, 3012, 2918, 1686, 1602, 1479, 1294, 1208, 1016, 861. ^{1}H NMR (400 MHz, DMSO-d$_6$/TMS) δ(ppm): 1.90 (12H, s, Me), 2.10 (12H, s, Me), 6.07 (2H, s, Ar$_3$CH), 6.25 (4H, s, OH), 6.52 (2H, s, 3-H DMP), 6.61 (4H, m, 2,6-H aldehyde), 6.72 (4H, s, 5-H DMP), 7.77 (2H, m, 3,5-H aldehyde), 7.94 (2H, m, 3,5-H aldehyde). ^{13}C NMR (100 MHz, DMSO-d$_6$/TMS) δ(ppm): 16.41, 17.20, 20.56, 20.95, 43.28, 114.88, 123.88, 124.32, 124.68, 127.30, 127.61, 128.29, 129.19, 129.81, 130.28, 131.58, 132.02, 141.99, 150.66, and 153.50. Anal. Calcd for $C_{40}H_{42}O_4$: C, 81.88; H, 7.21%. Found: C, 81.82; H, 7.20%.

6,6′-((4-nitrophenyl)methylene)bis(2,4-di-*tert*-butylphenol) (Table 2, Compound **3o**): mp: 153-155 °C; IR (KBr): ν (cm^{-1}) 3491, 2959, 1690, 1598, 1522, 1474, 1417, 1350, 1188, 116, 862. ^{1}H NMR (400 MHz, DMSO-d$_6$/TMS) δ(ppm): 1.05 (18H, s, *tert*-butyl), 1.33 (18H, s, *tert*-butyl), 6.28 (1H, s, Ar$_3$CH), 6.47 (2H, s, OH), 7.13 (2H, s, 3-H DMP), 7.13 (2H, d, *J=8 Hz*, 2,6-H aldehyde), 7.70 (2H, s, 5-H DMP), 8.13 (2H, d, *J=8 Hz*, 3,5-H aldehyde). ^{13}C NMR (100 MHz, DMSO-d$_6$/TMS) δ(ppm): 30.35, 31.70, 34.27, 35.16, 44.12, 121.76, 123.47, 125.08,

130.50, 130.64, 137.52, 141.46, 146.18, 151.02, and 153.25. Anal. Calcd for $C_{35}H_{47}NO_4$: C, 77.03; H, 8.68; N, 2.57%. Found: C, 77.07; H, 8.61; N, 2. 59%.

6,6′-((3-nitrophenyl)methylene)bis(2,4-di-*tert*-butylphenol) (Table 2, Compound **3p**): mp: 118-120 °C; IR (KBr): ν (cm^{-1}) 3528, 2959, 1530, 1473, 1350, 1186, 1023, 884. ^{1}H NMR (400 MHz, DMSO-d$_6$/TMS) δ(ppm): 2.01 (6H, s, Me), 2.06 (6H, s, Me), 6.06 (1H, s, Ar$_3$CH), 6.29 (2H, s, OH), 6.93 (2H, s, 3-H DMP), 7.16 (1H, d, *J=8 Hz*, 6-H aldehyde), 7.55 (2H, m, 4,5-H aldehyde), 7.64 (2H, s, 5-H DMP), 8.12 (1H, s, 2-H aldehyde). Anal. Calcd for $C_{35}H_{47}NO_4$: C, 77.03; H, 8.68; N, 2.57%. Found: C, 76.97; H, 8.64; N, 2. 55%.

6,6′-methylenebis(2,4-dimethylphenol) (Table 2, Compound **3q**): mp: 105-107 °C; IR (KBr): ν (cm^{-1}) 3424, 3299, 2917, 1609, 1482, 1381, 1286, 1193, 1150, 855. ^{1}H NMR (400 MHz, DMSO-d$_6$/TMS) δ(ppm): 2.00 (6H, s, Me), 2.10 (6H, s, Me), 3.74 (2H, s, CH$_2$), 6.62 (2H, s, OH), 6.68 (2H, s, 3-H DMP), 8.25 (2H, s, 5-H DMP). Anal. Calcd for $C_{17}H_{20}O_2$: C, 79.65; H, 7.86%. Found: C, 79.62; H, 7.79%.

6,6′-((2-methylpropyl)methylene)bis(2,4-dimethylphenol) (Table 2, Compound **3t**): mp: 160-163 °C; IR (KBr): ν (cm^{-1}) 3380, 3300, 2951, 2916, 1604, 1480, 1367, 1226, 1184, 1020, 858, 617. ^{1}H NMR (400 MHz, DMSO-d$_6$/TMS) δ(ppm): 0.84 (6H, d, *J=7.8 Hz*, 2(Me)CH), 1.34 (1H, m, 2(Me)CH), 1.78 (2H, t, *J=7.8 Hz*, CH$_2$), 2.09 (6H, s, Me), 4.60 (1H, t, *J=7.8 Hz*, Ar$_3$CH), 6.65 (2H, s, OH), 6.81 (2H, s, 3-H DMP), 8.25 (2H, s, 5-H DMP). Anal. Calcd for $C_{21}H_{28}O_2$: C, 80.73; H, 9.03%. Found: C, 80.69; H, 8.99%.

6,6′-((*n*-butyl)methylene)bis(2,4-dimethylphenol) (Table 2, Compound **3u**): mp: 140-143 °C; IR (KBr): ν (cm^{-1}) 3477, 3295, 2951, 2919, 1479, 1288, 1154, 1019, 857. ^{1}H NMR (400 MHz,

DMSO-d$_6$/TMS) δ(ppm): 0.80 (3H, m, CH$_3$-aldehyde), 1.13 (2H, m, CH$_2$-aldehyde), 1.25 (2H, m, CH$_2$-aldehyde), 1.88 (2H, m, CH$_2$-aldehyde), 2.08 (6H, s, Me), 4.49 (1H, t, *J=7.8 Hz*, Ar$_3$CH), 6.65 (2H, s, OH), 6.79 (2H, s, 3-H DMP), 8.20 (2H, s, 5-H DMP). Anal. Calcd for C$_{21}$H$_{28}$O$_2$: C, 80.73; H, 9.03%. Found: C, 80.76; H, 9.09%.

Results and Discussion

The importance of antioxidants in preventive medicine, food chemistry, and propellants are recognized since several years. Due to the significance of the described compounds, our plan of constructing 6,6′-(aryl(alkyl)methylene)bis(2,4-dialkylphenol) antioxidants has been done through one-pot and pseudo-three-component reaction from 2,4-dialkylphenol and various aromatic and aliphatic aldehydes under microwave irradiation in water (Scheme 1).
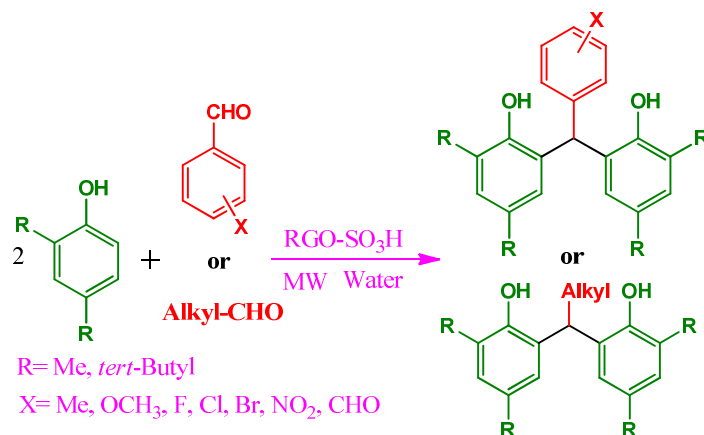
Scheme 1. Synthesis of bisphenolic antioxidants.

Preparation of catalyst

To prove our plan, it was prepared the RGO-SO$_3$H as outlined in Scheme 2 according the previously reported by Xiao et al. with a few modification.[52] First natural graphite which is

commercially available was converted to graphite oxide using sodium nitrate, H_2SO_4, and potassium permangenante.[51] This step introduced oxygen containing groups for example epoxy, hydroxyl, and carboxylic acid groups on the surface of graphite. After that, the graphite oxide was sonicated (45 w) for 15 min to produce GO nanosheets. For preparation of RGO-SO_3H, the prepared RGO using $NaBH_4$ as reducing agent was treated with H_2SO_4 (100 %) to afford RGO-SO_3H. The RGO-SO_3H was employed in synthesis of 6,6′-(aryl(alkyl)methylene)bis(2,4-dialkylphenol) antioxidants in water under microwave irradiation.
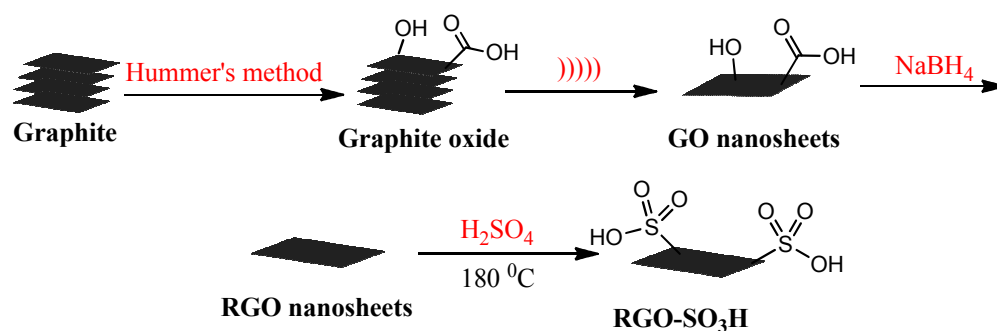
Scheme 2. Synthetic route for preparation of catalyst.

Characterization of RGO-SO₃H

After successful preparation of the RGO-SO_3H, the catalyst was characterized by some microscopic and spectroscopic techniques including FESEM, TEM, AFM, FT-IR and Raman spectroscopy, XRD, TGA, and back acid-base titration.

To investigate the morphology of the prepared catalyst, FESEM images were taken for the GO, and RGO-SO_3H. The transparent and flake-like sheets of the prepared GO nanosheets are observed in Figure 2a. Figure 2a was found that GO nanosheets consists of randomly aggregated and crumpled thin sheets which also observed with wrinkles and folds on the surface of GO nanosheets. This result confirmed that two dimensional GO nanosheets can be produced from

exfoliation of suspended graphite oxide. The Figure 2b revealed that the presence of functional groups on the surface of GO are carried out, which is quite different morphology from the pristine GO nanosheets. Figures 2c and 2d exhibit the TEM images of GO and RGO nanosheets respectively. In these images, it seems that the GO and RGO exhibit a typical exfoliated and two-dimensional nanosheets with a rather and large flat and smooth flake-like morphology with several layers. In addition, they reveal that two-dimensional flake-like of pristine graphite is still in GO and RGO nanosheets after Hummer's method.
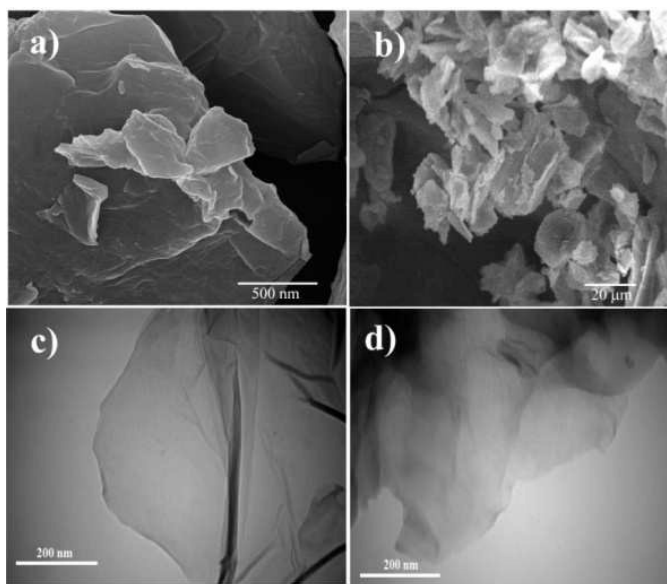
Figure 2. FESEM images of a) GO nanosheets b) RGO-SO$_3$H and TEM images of c) GO nanosheets d) RGO.

As shown in Figure 3a, the AFM analysis reveals that the measured values of thickness are in the range 0.9-1.5 nm, indicating that exfoliated mono- and di-layer graphene oxide was obtained in this study. These GO layers should be mostly mono-layered, although these amount are somewhat larger than the interlayer spacing (0.78 nm) of the parent GO. The sheets are a little more 'bumpy' than predicted, which is possibly due to the existence of abundant functional

groups, such as carboxylic, epoxy, and hydroxyl groups, bonded to both sides of the GO sheets, which disrupts the original conjugation and introduces lattice defects to result in folds and distortions on the sheets. After reduction of GO with $NaBH_4$, the process of sulfonation was done and the AFM analysis of the $RGO-SO_3H$ was provided (Figure 3b). As shown in this Figure, the measured values of thickness in $RGO-SO_3H$ was increased and the range of 2.4-4.1 nm indicating that the process of functionalization was successfully occurred and the functional groups were immobilized on the surface of RGO. According to the hydrogen bonding between the layers of $RGO-SO_3H$, the prepared catalyst was three to seven layers of graphene sheets.
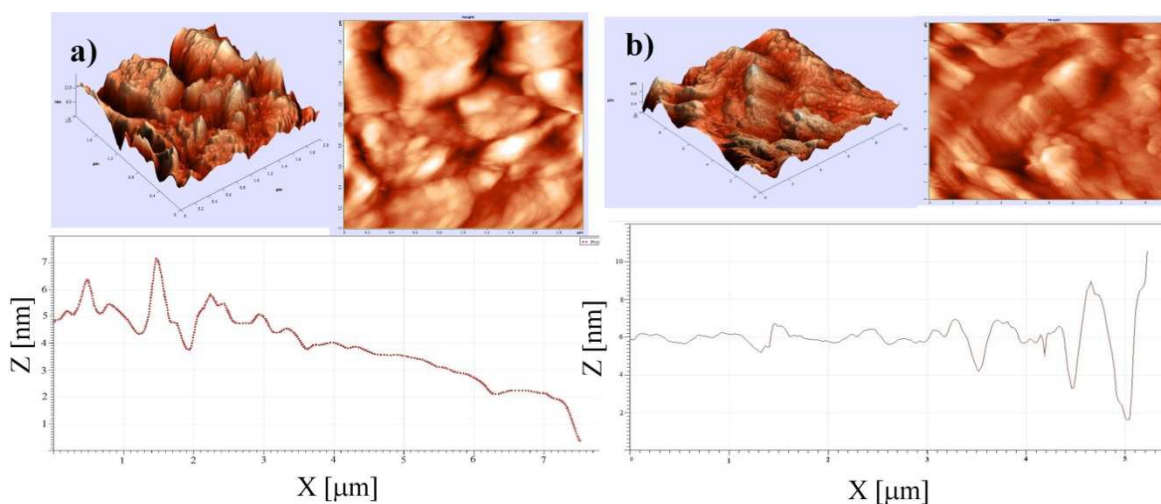
Figure 3. AFM images of a) GO nanosheets b) $RGO-SO_3H$

Figure 4a-d shows the FT-IR spectra of graphite, GO, RGO, and $RGO-SO_3H$ respectively. The high symmetry introduced to pristine graphite generates very weak infrared peaks due to the weak difference of charge states and very small induced electric dipole. The peak related to carbon-carbon double bonds at 1573 cm^{-1} is not sharp in the spectrum of graphite (Figure 4a). The FT-IR spectrum of GO was shown in Figure 4b.The process of Hummer's method and sonication process breaks the symmetry of graphite. The peak at approximately 1580 cm^{-1} is

attributed to carbon-carbon double bonds. This peak is sharper than graphite due to the un-symmetry of GO. Also, this spectrum shows the peaks at 1064, 1719, and 3394 cm^{-1} which could be assigned to carbon-oxygen, carbonyl, and hydroxyl stretching mode of functional groups such as hydroxyl, carboxylic, and epoxy groups attachment to GO respectively. The chemical reduction of GO with NaBH$_4$ produce RGO that the FT-IR spectrum of RGO is shown in Figure 4c. This spectrum shows that the peaks of the hydroxyl and carbonyl groups were disappeared due to the used NaBH$_4$ as reducing agent. The peak at 3423 cm^{-1} is related to presence of water on KBr pellets. Also, the presence of the peak at 1566 cm^{-1} show that after chemical reduction at 100 °C for 24 h, the RGO is still flake-like sheets. At the end of this image, Figure 4d shows FT-IR spectrum of RGO-SO$_3$H. H$_2$SO$_4$ treatment also results in the appearance of the peaks at about 1384 and 1215 cm^{-1}, which corresponds to the SO$_2$ symmetric and asymmetric stretching modes respectively. In addition, in the low frequency part of spectrum the line at 605 cm^{-1} was assigned to carbon-sulfur stretching mode, suggesting the existence of covalent sulfonic acid groups on the surface of GO nanosheets.
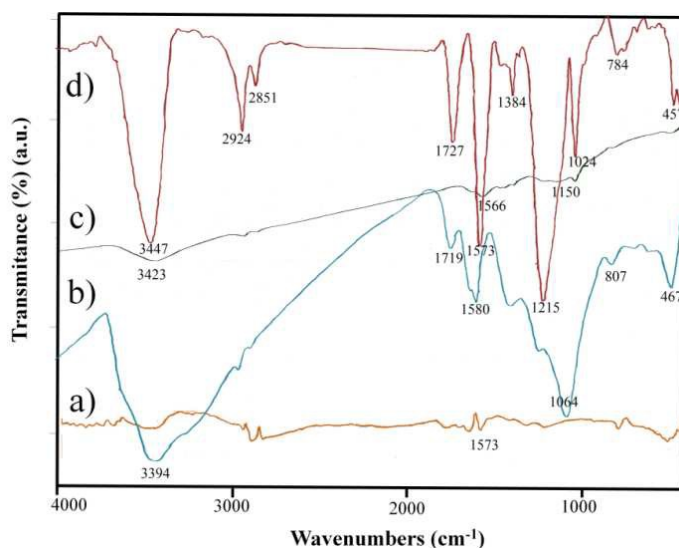

Figure 4. FT-IR spectra of a) graphite b) GO c) RGO d) RGO-SO$_3$H.

Figure 5a-d shows XRD patterns of graphite, GO, RGO, and G-SO$_3$H respectively. The XRD pattern of graphite (Figure 5a) shows a diffraction peak at approximately $2\theta= 26.5°$ corresponding to the interlayer spacing (*d*-spacing). After to do Hummer's method, the peak at about $2\theta= 26.5°$ was broad peak and the peak at $2\theta= 12°$ was appeared. The interlayer spacing (*d*-spacing) of GO was calculated 0.78 nm which revealed the introduction of oxygen species on graphene network sheets (Figure 5b).[53] After chemical reduction of exfoliated GO with NaBH$_4$, the diffraction peak of GO at $2\theta= 12°$ disappeared and a broad peak at about $2\theta= 24°$ was observed, indicating the fully reduction and exfoliation of GO and the production of RGO nanosheets.[54] As shown in Figure 5c in the RGO nanosheets was rather broad peak and significantly different from that observed for graphite ($2\theta= 26.5°$). Figure 4d shows XRD pattern of RGO-SO$_3$H after hydrothermal sulfonation. The XRD pattern (Figure 5d) has very similar peaks to RGO suggesting their similar graphene layers.
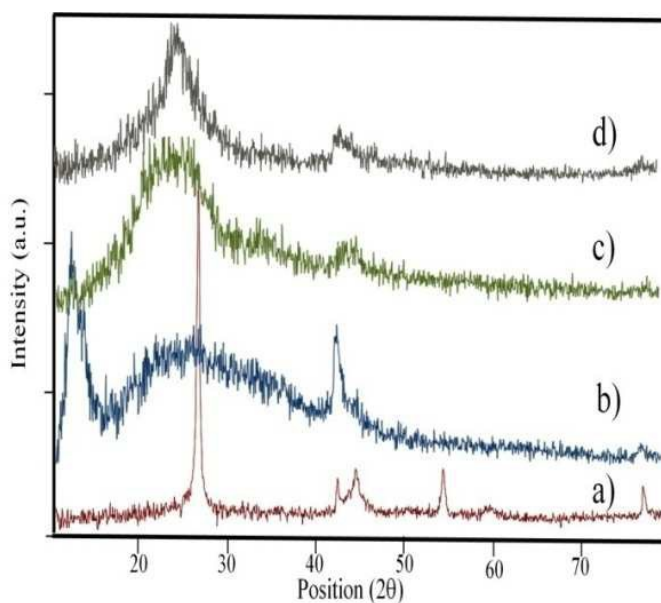
Figure 5. XRD pattern of a) graphite b) GO c) RGO d) RGO-SO$_3$H.

Raman spectroscopy is strongly sensitive to the structure of graphene and it has proved to be an essential tool to characterize graphene. Typical Raman spectrum of GO nanosheet is shown in Figure 6. The D-band is related to disorder induced scattering resulting from imperfection of disorder graphene. The G-band is associated with an E_{2g} mode of graphite and is related to vibration of *sp²* bonded carbon hybridize in a two dimensional graphite. The D band appears at about 1347 cm⁻¹, and the G band appears at approximately 1593 cm⁻¹. The G-band arises from the stretching of the carbon-carbon bond in graphitic materials, and is related to *sp²* carbon systems. The D-band is caused by disordered structure of graphene. The other Raman bands are at 2717 cm⁻¹ (2D band), and 2931 cm⁻¹ (D+G-band).[55]
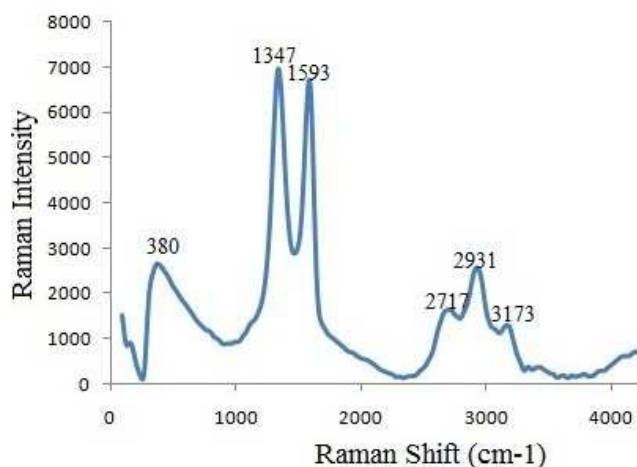
Figure 6. Raman spectrum of GO.

TGA analysis curves of GO and RGO-SO$_3$H are compared in Figure 7. Both curves show similar characteristics. As shown in Figure 7a, the weight loss (8%) before 160 °C is caused by the release of trapped water between GO nanosheets.[56] The weight loss (23%) between 160 °C and 260 °C is attributed to the decomposition of less stable functional groups for example hydroxyl, carboxylic acid, and epoxy on the surface of GO nanosheets.[57] The presence of sulfonated groups

20

on RGO nanosheets were further analyzed by TGA (Figure 7b). A little weight loss (8%) before

176 °C is attributed to the trapped water. For the prepared catalyst, there is a slow decrease of

weight (46%) when the temperature is between 400 °C and 580 °C that is attributed to sulfonated

groups. Thermogravimetric analysis can estimate account of functional groups per carbon

atoms.[58] To calculate the extent of functionalization, weight loss values were employed together

with the molecular weight of the different groups and the following equation was applied.

$$X = \frac{R\,(\%) \times Mw\,(\frac{g}{mol})}{L\,(\%) \times 12\,(\frac{g}{mol})}$$

Where X stands for the number of carbon atoms in RGO-SO$_3$H per each covalent functional

group, R (%) is the residual mass at 580 °C in the TGA plot, L (%) is the weight loss in the range

of 176°C and 580 °C, and Mw is the molecular weight of the sulfonated groups. In according to

the above equation, taking in to account that the sulfonated groups measurement indicated that

one functionality every approximately thirty four carbon atoms.
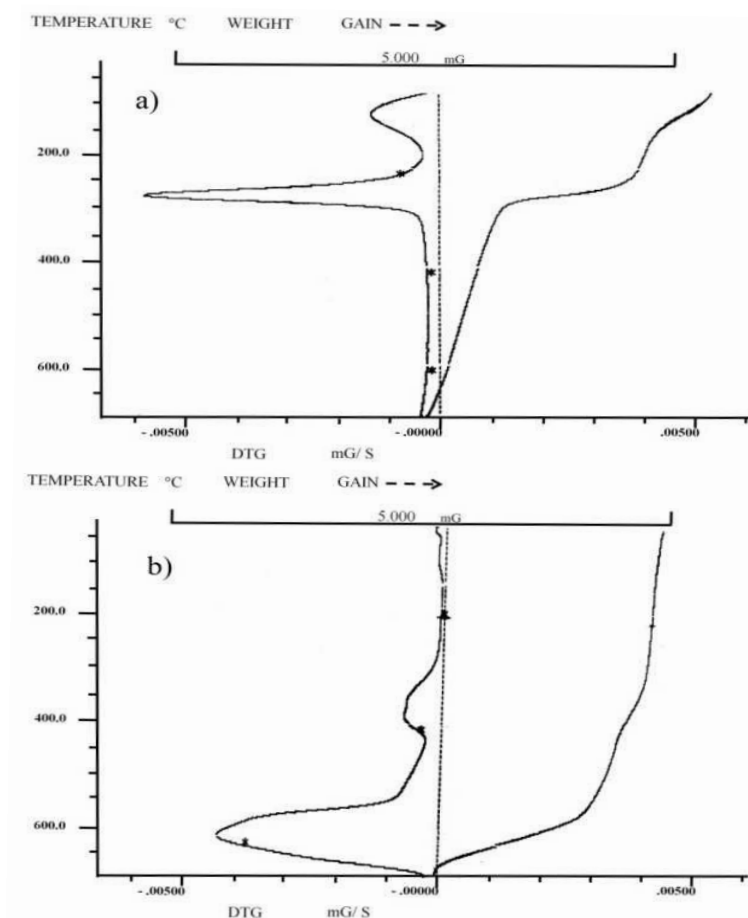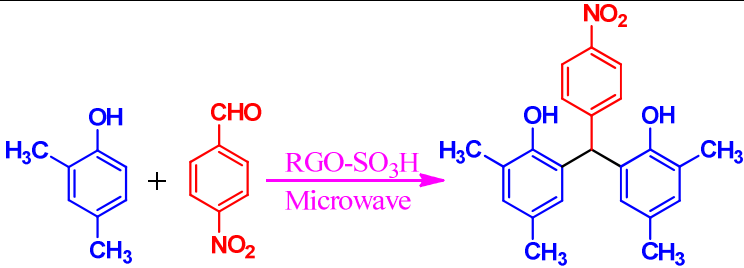
Figure 7. Thermogravimetric analysis of a) GO b) RGO-SO$_3$H.

The density of SO$_3$H groups on the RGO was determined by back acid-base titration and solution of NaCl. The back acid-base titration showed that the amount of SO$_3$H attached to RGO is 2.15 mmol. g^{-1}. Also, the solution of NaCl determined the amount of sulfonated groups is 2.15 mmol. g^{-1}.

Catalytic evaluation of RGO-SO$_3$H in the synthesis of bisphenolic antioxidants under microwave irradiation

The prepared RGO-SO$_3$H was used as heterogeneous catalysts in the synthesis of 6,6′-(aryl(alkyl)methylene)bis(2,4-dialkylphenol) antioxidants. To optimize the reaction conditions

for the formation of 6,6′-(aryl(alkyl)methylene)bis(2,4-dialkylphenol) antioxidants from 2,4-dialkylphenol and aromatic and aliphatic aldehydes, we devoted our efforts on this research using the reaction of 2,4-dimethylphenol (**1**) and 4-nitrobenzaldehyde (**2a**) in the catalytic amount of the RGO-SO$_3$H as a simple model reaction under microwave irradiation in the presence of various reaction conditions including catalyst amount, different solvent, and power of microwave oven (Table 1). Choosing an appropriate solvent has crucial importance for the successful microwave-promoted in organic synthesis. To observe for optimal solvents, the model reaction was carried out in different solvents such as EtOH, CH$_3$CN, H$_2$O, and without any solvent (Table 1, entries 1-4). As shown in Table 1, entry 3 gave the best result for medium of the model reaction. Therefore, water solvent was chosen as a reaction medium. Among the different solvent alternatives in organic chemistry, water is extremely cheap and nontoxic. In addition to these two general advantages, several benefits for the reaction are expected when using water as a reaction medium for microwave-promoted approach. For example water is rapidly heated by microwave irradiation to high reaction temperature, enabling water to act as less polar pseudo-organic solvent.[59] For optimization of microwave oven power, an increase in power of microwave (100 to 450 W) led to decrease time of the model reaction and increased yields of the desired products. At 300 W the yield and time of the model reaction were 96% and 9 min respectively and it similar at 450 W (Table 1, entries 5-7). In addition, we examined the model reaction in different amounts of the catalyst (Table 1, entries 8-10). The best result was obtained with 30 mg of the RGO-SO$_3$H.

Table 1. Optimizing the reaction conditions.[a]

Entry	RGO-SO₃H (mg)	Solvent	Power (W)	Time (min)	Yield (%)[b]
1	30	EtOH	100	18	67
2	30	CH₃CN	100	17	70
3	30	H₂O	100	15	83
4	30	Solvent free	100	17	80
5	30	H₂O	180	15	85
6	30	H₂O	300	9	96
7	30	H₂O	450	8	95
8	25	H₂O	300	11	92
9	35	H₂O	300	9	96
10	-	H₂O	300	40	20

a) General reaction conditions: 2,4-dimethylphenol (1) (6 mmol), 4-nitrobenzaldehyde (2a) (2 mmol), solvent (5-7 mL).

b) Isolated yields.

As shown in Table 2, a range of aromatic and aliphatic aldehydes were employed in order to show the applicability and merit of this approach in the synthesis of bisphenolic antioxidants. In order to generalize optimum reaction conditions, different derivatives of 6,6′-(aryl(alkyl)methylene)bis(2,4-dialkylphenol) antioxidants (**3a-3v**) were synthesized from the one-pot reaction of 2,4-dialkylphenols and aromatic or aliphatic aldehydes (**2a-2v**) in the presence of catalytic amount of RGO-SO₃H (30 mg), at power 300 W in water under microwave irradiation. The reaction smoothly proceeded to give the corresponding bisphenolic antioxidants in excellent yields and short reaction times relative to classical thermal conditions. As shown in Table 2, the aromatic aldehydes with electron-withdrawing groups on the *ortho-* or *para-* positions accelerate the time of the reaction and improved the yield of desired products compared with the electron-donating groups on *ortho-* or *para-* positions. As can be seen in Table 2, entry

14, the practical synthetic efficiency of this protocol was studied by reaction of 4-formylbenzaldehyde (**2n**) with 2,4-dimethylphenol in the presence of the RGO-SO$_3$H. We observed the both of the carbonyl groups on the aromatic ring of **2n** were reacted with 2,4-dimethylphenol.

Some of the five membered ring heteroaromatic aldehydes such as furfural and pyrrole-2-carboxaldehyde were used in the synthesis of target products (Table 2, entries 18, 19). In these experiments, the target molecules were not obtained but the polymerization of furfural and pyrrole-2-carboxaldehyde were happened under microwave and thermal conditions before the production of the compounds **3r** and **3s**. The pyrrole and furane which in fact protonated preferably at a ring carbon in acidic conditions, and which is polymerized under such conditions presumably by attack of a nonprotonated pyrrole or furane aldehydes upon its conjugated acid.[60, 61] Therefore, the protonation of carbonyl group on the furfural and pyrrole-2-carboxaldehyde do not occurred. Also, it was tried that the reaction was carried out in the absence of RGO-SO$_3$H, but any target products observed.
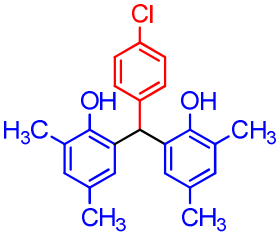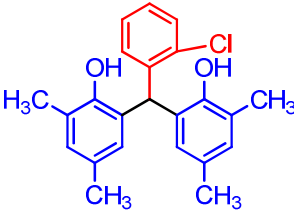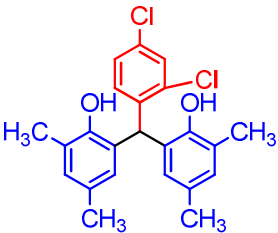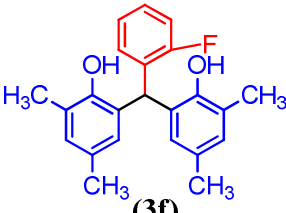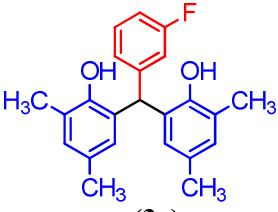
In continuous of this part, we report on another application of aliphatic aldehydes for the synthesis of bisphenolic antioxidants (Table 2, entries 20-22). As shown in these entries, this protocol worked well when pentanal and 3-methylbutyraldehyde were employed and the compounds **3t**, and **3u** were produced in 88% and 86% respectively in water under microwave irradiation. When it was used isobutyraldehyde, the final product was observed only in 10%, because the steric hindrance of isopropyl groups do not allow that the benzene ring attack to the electrophilic carbon of aldehyde (Table 2, entry 22).
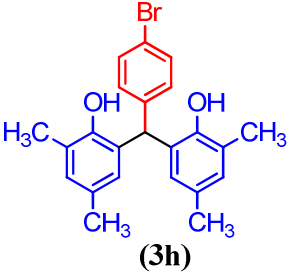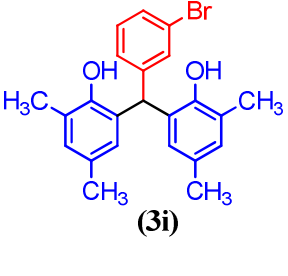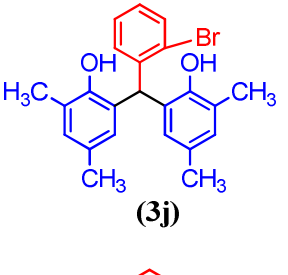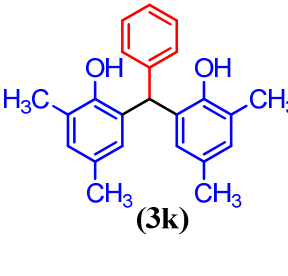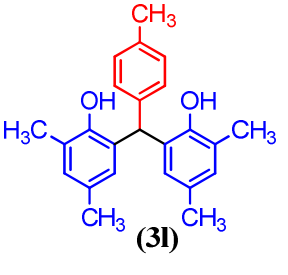
Also, we performed the reaction for the synthesis of bisphenolic antioxidants under conventional thermal conditions. By comparison of the obtained results using microwave
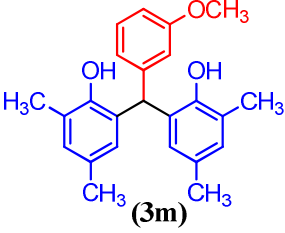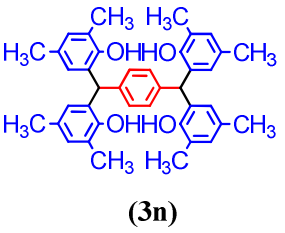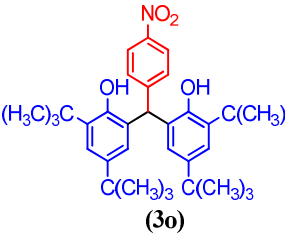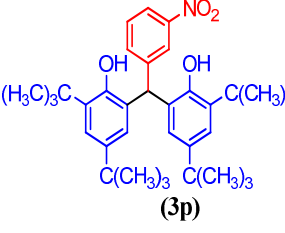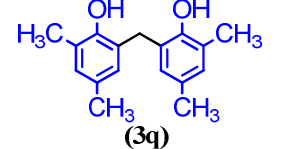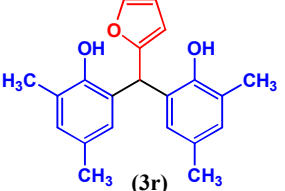
irradiation with conventional thermal method, it can be concluded that the reaction time was dramatically reduced and the yield of the desired products were better. Also, for all of the derivatives, TOF and TON of the catalyst were better in microwave conditions. Therefore, microwave irradiation method reveals several worthwhile advantages over conventional thermal by significantly reducing time of the reaction and increasing yield of the products.
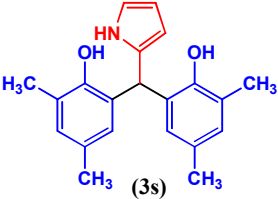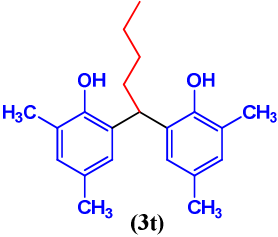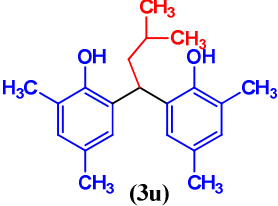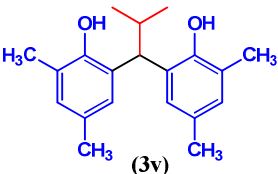
Table 2. Synthesis of 6,6′-(aryl(alkyl)methylene)bis(2,4-dialkylphenol) antioxidants under different conditions

Entry	R	X	Product	Microwave method [a]				Thermal method [b]			
				Time (min)	Yield (%)[c]	TOF $(h^{-1})^f$	TON[g]	Time (min)	Yield (%)[c]	TOF $(h^{-1})^f$	TON[g]
1	CH_3	4-NO_2	(3a)	7	96	256	29	40	92	31	21
2	CH_3	3-NO_2	(3b)	9	95	193	29	45	93	28	21

3	CH$_3$	4-Cl	(3c)	6	98	300	30	30	90	42	21	
4	CH$_3$	2-Cl	(3d)	8	93	223	29	30	94	44	22	
5	CH$_3$	2-Cl, 4-Cl	(3e)	6	94	290	29	25	89	50	21	
6	CH$_3$	2-F	(3f)	10	89	159	27	40	82	28	19	
7	CH$_3$	3-F	(3g)	11	87	150	27	30	90	42	21	

8	CH$_3$	4-Br		5	98	375	30	20	95	67	22
9	CH$_3$	3-Br		8	96	231	30	30	88	40	20
10	CH$_3$	2-Br		9	91	187	28	15	89	84	21
11	CH$_3$	H		12	90	140	28	60	80	19	19
12	CH$_3$	4-CH$_3$		11	89	155	28	60	81	19	19

(3h)

(3i)

(3j)

(3k)

(3l)

13	CH$_3$	3-OCH$_3$	**(3m)**	14	88	117	27	50	78	11	9
14[d]	CH$_3$	4-CHO	**(3n)**	12	90	140	28	30	82	38	19
15	*tert*-butyl	4-NO$_2$	**(3o)**	11	93	161	29	60	89	21	21
16	*tert*-butyl	3-NO$_2$	**(3p)**	9	91	187	28	50	90	25	21
17[e]	CH$_3$	Formalde hyde [i]	**(3q)**	5	96	375	30	10	96	129	22
18[h]	CH$_3$	Furane-2-aldehyde [i]	**(3r)**	10	--	--	--	20	--	--	--

19[h]	CH$_3$	Pyrrole-2-aldehyde [i]	(3s)	10	--	--	--	20	--	--	--
20	CH$_3$	Pentanal [i]	(3t)	8	88	308	41	35	80	48	28
21	CH$_3$	3-Me-butanal [i]	(3u)	7	86	342	40	45	79	36	27
22	CH$_3$	2-Me-propanal [i]	(3v)	20	<10	15	5	90	<10	2.3	3.4

a) Microwave conditions: 2,4-dialkylphenol (**1**) (6 mmol), aldehyde (**2a-2v**) (2 mmol), H$_2$O (5-7 mL), Power= 300 W, RGO-SO$_3$H (30 mg).

b) Thermal conditions: 2,4-dialkylphenol (**1**) (6 mmol), aldehyde (**2a-2v**) (2 mmol), solvent free, T= 100 °C, RGO-SO$_3$H (40 mg).

c) Isolated yields.

d) Reaction conditions: 2,4-dimethylphenol (12 mmol), therphthaldehyde (**2n**) (2 mmol).

e) Reaction conditions: 2,4-dimethylphenol (4 mmol), paraformaldehyde (**2q**) (2 mmol).

f) TOF (h^{-1}) = (mmol of product / mmol of active site of catalyst) / Time of the reaction (h)

g) TON = mmol of product / mmol of active site of catalyst

h) The reaction was also performed in the absence of catalyst, but was not obtained any final product.

i) In these entries, the complete names of aldehydes are presented.

The proposed reaction mechanism for solid acid catalyst based-graphene nanosheets catalyzed synthesis of 6,6′-(aryl(alkyl)methylene)bis(2,4-dialkylphenol) antioxidants using 2,4-dialkylphenol and different aldehydes are shown in Scheme 3.
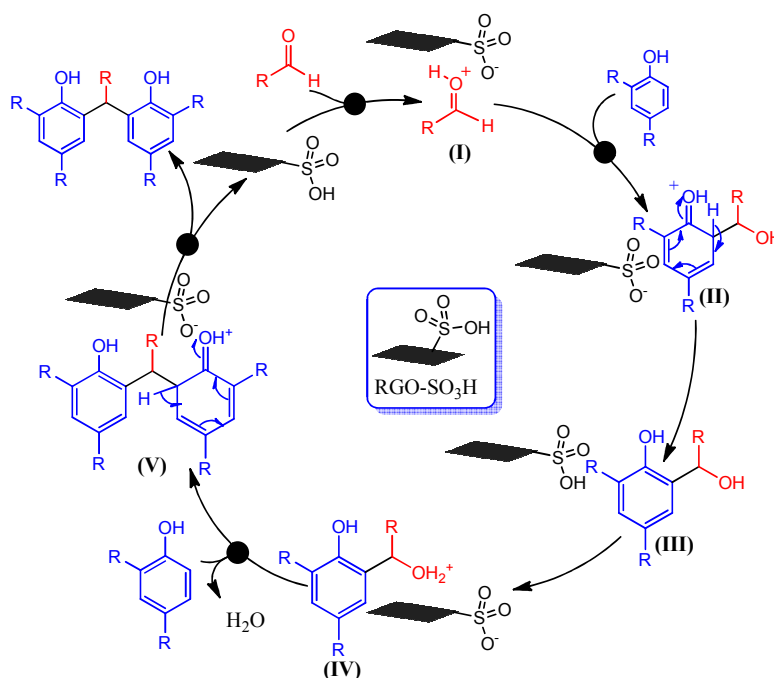
Scheme 3. The proposed reaction pathway.

The reaction proceeds via a series of protonic shifts from catalysts to the substrates. First, the aldehydes are activated by protonation with solid acid catalysts to give species (**I**). Nucleophilic attack of 2,4-dialkylphenol on (**I**) affords species (**II**) and (**III**) which in turn is activated by solid acid catalysts to afford species (**IV**). Nucleophilic attack of the next molecule of 2,4-dialkylphenol to species (**IV**), gives (**V**) which is subsequently converted to 6,6′-(aryl(alkyl)methylene)bis(2,4-dialkylphenol) antioxidants and releases solid acid catalysts for the next catalytic runs.

Figure 8 shows the robustness and recyclability of the RGO-SO₃H after seven runs. The RGO-SO₃H started to display a gradual decrease in catalytic activity after multiple cycles. The RGO-SO₃H was investigated by simple separation of the catalyst from the reaction of 2,4-dimethylphenol and 4-bromobenzaldehyde (**2h**). At the end of each reaction, the solid acid catalyst was isolated by simple filtration under reduced pressure, washed exhaustively with

deionized water, *n*-hexane, and ethanol, and dried at 100 °C for 24 h before being used with fresh
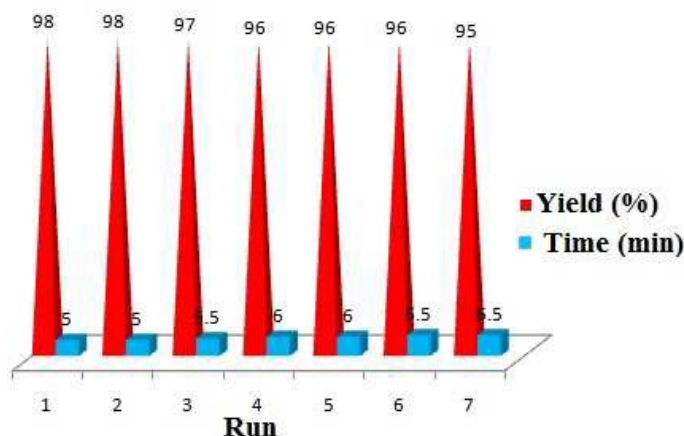
2,4-dimethylphenol and **2h**.

Figure 8. Reusability of RGO-SO$_3$H in the synthesis of **3h** under microwave irradiation.

As shown in Figure 8, in the first cycle the yield of **3h**, and time of the formation **3h**, were 98%,

and 5 min, respectively. Then, the RGO-SO$_3$H was used at multiple sequential runs. The results

show that the yield of **3h** and time of the reaction only were 95%, and 6.5 min respectively.

Conclusions

To conclude, we have established that the RGO-SO$_3$H is a robust, reusable, and heterogeneous

solid acid catalyst for the synthesis of bisphenolic antioxidants in water under microwave

irradiation. In addition, we carried out the reaction for the synthesis of bisphenolic antioxidants

under thermal conditions. By comparison of the obtained results using thermal method with

microwave methods we can be concluded the reaction time was dramatically reduced and the

yield of products were increased. Therefore, microwave irradiation method exhibits several

worthwhile benefits over thermal conditions. Also, in this study, the prepared catalyst was

characterized by some microscopic and spectroscopic techniques such as FESEM, TEM, AFM,

FT-IR and Raman spectroscopy, XRD, TGA and back acid-base titration. The microscopic and spectroscopic analysis was confirmed that the functionalization of RGO was performed. The back acid-base titration was shown that the total density of sulfonated groups on the surface of RGO was 2.15 mmol.g^{-1}. In addition, the reusability and stability of the RGO-SO$_3$H was investigated in the various reaction runs and confirmed.

Acknowledgements

References

1.   J. Wollgast and E. Anklam, *Food Res. Int.*, 2000, **33**, 423-447.

2.   T. Mesganaw and N. K. Garg, *Org. Process Res. Dev.*, 2012, **17**, 29-39.

3.   C. Stockley, P.-L. Teissedre, M. Boban, C. Di Lorenzo and P. Restani, *Food Funct.*, 2012, **3**, 995-1007.

4.   Y.-J. Guo, G.-F. Deng, X.-R. Xu, S. Wu, S. Li, E.-Q. Xia, F. Li, F. Chen, W.-H. Ling and H.-B. Li, *Food Funct.*, 2012, **3**, 1195-1205.

5.   I. Hasegawa, T. Nakamura, S. Motojima and M. Kajiwara, *J. Mater. Chem.*, 1995, **5**, 193-194.

6.   J. S. Weinger and S. A. Strobel, *Biochemistry*, 2006, **45**, 5939-5948.

7.   S. F. Parker, *Chem. Commun.*, 2011, **47**, 1988-1990.

8.   F. Niu, C.-C. Liu, Z.-M. Cui, J. Zhai, L. Jiang and W.-G. Song, *Chem. Commun.*, 2008, 2803-2805.

9. G. C. G. Martinez-Avila, A. F. Aguilera, S. Saucedo, R. Rojas, R. Rodriguez and C. N. Aguilar, *Cr. Rev. Food Sci.*, 2012, **54**, 303-311.

10. R. L. Webster, P. M. Rawson, D. J. Evans and P. J. Marriott, *Energ. Fuel.*, 2014, **28**, 1097-1102.

11. F. A. V. Sallivan and G. Conn, *U. S. Patent*, 1957, 2, 796, 445.

12. S. Saito, T. Ohwada and K. Shudo, *J. Am. Chem. Soc.*, 1995, **117**, 11081-11084.

13. R. Goossens, M. Smet and W. Dehaen, *Tetrahedron Lett.*, 2002, **43**, 6605-6608.

14. S. K. Jana, T. Okamoto, T. Kugita and S. Namba, *Appl. Catal. A: General*, 2005, **288**, 80-85.

15. V. Nair, K. G. Abhilash and N. Vidya, *Org. Lett.*, 2005, **7**, 5857-5859.

16. J. Esquivias, R. Gómez Arrayás and J. C. Carretero, *Angew. Chem.Int. Ed.*, 2006, **45**, 629-633.

17. S. Podder, J. Choudhury, U. K. Roy and S. Roy, *J. Org. Chem.*, 2007, **72**, 3100-3103.

18. Z. Li, Z. Duan, J. Kang, H. Wang, L. Yu and Y. Wu, *Tetrahedron*, 2008, **64**, 1924-1930.

19. S. Genovese, F. Epifano, C. Pelucchini and M. Curini, *Eur. J. Org. Chem.*, 2009, **2009**, 1132-1135.

20. C. V. Rode, A. C. Garade and R. C. Chikate, *Catal. Surv. Asia*, 2009, **13**, 205-220.

21. K. Shimizu, S. Kontani, S. Yamada, G. Takahashi, T. Nishiyama and A. Satsuma, *Appl. Catal. A: General*, 2010, **380**, 33-39.

22. I. Mohammadpoor-Baltork, M. Moghadam, S. Tangestaninejad, V. Mirkhani, K. Mohammadiannejad-Abbasabadi and M. A. Zolfigol, *C. R. Chimie*, 2011, **14**, 934-943.

23. S. Rostamizadeh, N. Zekri and L. Tahershamsi, *Polycycl. Aromat. Comp.*, 2014, **34**, 542-560.

24. R. Fareghi-Alamdari, M. Golestanzadeh, F. Agend and N. Zekri, *Can. J. Chem.*, 2013, **91**, 982-991.

25. Y. Nabae, J. Liang, X. Huang, T. Hayakawa and M.-a. Kakimoto, *Green Chem.*, 2014, **16**, 3596-3602.

26. E. Kolvari, N. Koukabi and O. Armandpour, *Tetrahedron*, 2014, **70**, 1383-1386.

27. A. B. Atar and Y. T. Jeong, *Tetrahedron Lett.*, 2013, **54**, 1302-1306.

28. A. B. Atar, J. S. Kim, K. T. Lim and Y. T. Jeong, *New J. Chem.*, 2015, **39**, 396-402.

29. J. Liu, J. Tang and J. J. Gooding, *J. Mater. Chem.*, 2012, **22**, 12435-12452.

30. X. Peng, L. Peng, C. Wu and Y. Xie, *Chem. Soc. Rev.*, 2014, **43**, 3303-3323.

31. R. Raj, S. C. Maroo and E. N. Wang, *Nano Lett.*, 2013, **13**, 1509-1515.

32. A. B. Seabra, A. J. Paula, R. de Lima, O. L. Alves and N. Durán, *Chem. Res. Toxic.*, 2014, **27**, 159-168.

33. S. M. Islam, A. S. Roy, R. C. Dey and S. Paul, *J. Mol. Catal. A: Chem.*, 2014, **394**, 66-73.

34. P. Fakhri, B. Jaleh and M. Nasrollahzadeh, *J. Mol. Catal. A: Chem.*, 2014, **383–384**, 17-22.

35. S. Liu, J. Tian, L. Wang and X. Sun, *Carbon*, 2011, **49**, 3158-3164.

36. S. Liu, J. Tian, L. Wang, H. Li, Y. Zhang and X. Sun, *Macromolecules*, 2010, **43**, 10078-10083.

37. Z. Xing, Q. Chu, X. Ren, J. Tian, A. M. Asiri, K. A. Alamry, A. O. Al-Youbi and X. Sun, *Electrochem. Commun.*, 2013, **32**, 9-13.

38. Y. Zhang, J. Tian, H. Li, L. Wang, X. Qin, A. M. Asiri, A. O. Al-Youbi and X. Sun, *Langmuir*, 2012, **28**, 12893-12900.

39. H. Li, S. Liu, J. Tian, L. Wang, W. Lu, Y. Luo, A. M. Asiri, A. O. Al-Youbi and X. Sun, *ChemCatChem*, 2012, **4**, 1079-1083.

40. S. Horikoshi and N. Serpone, *Catal. Sci. Tech.*, 2014, **4**, 1197-1210.

41. J. K. S. Wan, *Res. Chem. Intermed.*, 1993, **19**, 147-158.

42. R. Ghahremanzadeh, Z. Rashid, A. H. Zarnani and H. Naeimi, *Appl. Catal. A: General*, 2013, **467**, 270-278.

43. H. Naeimi and M. Moradian, *Appl. Catal. A: General*, 2013, **467**, 400-406.

44. H. Naeimi and Z. Nazifi, *J. Nanopart. Res.*, 2013, **15**, 1-11.

45. H. Naeimi and L. Moradi, *Catal. Commun.*, 2006, **7**, 1067-1071.

46. R. Ghahremanzadeh, Z. Rashid, A.-H. Zarnani and H. Naeimi, *J. Ind. Eng. Chem.*, 2014, DOI: 10.1016/j.jiec.2013.1012.1109.

47. H. Naeimi and V. Nejadshafiee, *New J. Chem.*, 2014, **38**, 5429-5435.

48. H. Naeimi, Z. Rashid, A.-H. Zarnani and R. Ghahremanzadeh, *New J. Chem.*, 2014, **38**, 5527-5535.

49. H. Naeimi, Z. Rashid, A. H. Zarnani and R. Ghahremanzadeh, *New J. Chem.*, 2014, **38**, 348-357.

50. H. Naeimi and M. Golestanzadeh, *RSC Advances*, 2014, **4**, 56475-56488.

51. W. S. Hummers and R. E. Offeman, *J. Am. Chem. Soc.*, 1958, **80**, 1339-1339.

52. F. Liu, J. Sun, L. Zhu, X. Meng, C. Qi and F.-S. Xiao, *J. Mater. Chem.*, 2012, **22**, 5495-5502.

53. D. Long, W. Li, L. Ling, J. Miyawaki, I. Mochida and S.-H. Yoon, *Langmuir*, 2010, **26**, 16096-16102.

54. X. Fan, W. Peng, Y. Li, X. Li, S. Wang, G. Zhang and F. Zhang, *Adv. Mater.*, 2008, **20**, 4490-4493.

55. K. N. Kudin, B. Ozbas, H. C. Schniepp, R. K. Prud'homme, I. A. Aksay and R. Car, *Nano Lett.*, 2007, **8**, 36-41.

56. S. Eigler, C. Dotzer, A. Hirsch, M. Enzelberger and P. Müller, *Chem. Mater.*, 2012, **24**, 1276-1282.

57. M. J. McAllister, J.-L. Li, D. H. Adamson, H. C. Schniepp, A. A. Abdala, J. Liu, M. Herrera-Alonso, D. L. Milius, R. Car, R. K. Prud'homme and I. A. Aksay, *Chem. Mater.*, 2007, **19**, 4396-4404.

58. J. M. González-Domínguez, M. González, A. Ansón-Casaos, A. M. Díez-Pascual, M. A. Gómez and M. T. Martínez, *J. Physic. Chem. C*, 2011, **115**, 7238-7248.

59. X. Wu and M. Larhed, *Org. Lett.*, 2005, **7**, 3327-3329.

60. R. J. Abraham, E. Bullock and S. S. Mitra, *Can. J. Chem.*, 1959, **37**, 1859-1869.

61. G. F. Smith, in *Adv. Heterocycl. Chem.*, ed. A. R. Katritzky, Academic Press, 1963, vol. Volume 2, pp. 287-309.